# Multiple solutions in the theory of dc glow discharges

To cite this article: P G C Almeida *et al* 2010 *Plasma Sources Sci. Technol.* **19** 025019

Plasma Sources Sci. Technol. **19** (2010) 025019 (13pp) doi:10.1088/0963-0252/19/2/025019

# Multiple solutions in the theory of dc glow discharges

**P G C Almeida, M S Benilov and M J Faria**

Departamento de Física, Universidade da Madeira, Largo do Município, 9000 Funchal, Portugal

Received 28 May 2009, in final form 30 November 2009
Published 24 March 2010
Online at stacks.iop.org/PSST/19/025019

**Abstract**
Multiple steady-state solutions existing in the theory of dc glow discharges are computed for the first time. The simulations are performed in 2D in the framework of the simplest self-consistent model, which accounts for a single ion species and employs the drift–diffusion approximation. Solutions describing up to nine different modes were found in the case where losses of the ions and the electrons due to diffusion to the wall were neglected. One mode is 1D, exists at all values of the discharge current, and represents in essence the well-known solution of von Engel and Steenbeck. The other eight modes are axially symmetric, exist in limited ranges of the discharge current, and are associated with different patterns of current spots on the cathode. The mode with a spot at the centre of the cathode exhibits a well pronounced effect of normal current density. Account of diffusion losses affects the solutions dramatically: the number of solutions is reduced, a mode appears that exists at all discharge currents and comprises the Townsend, subnormal, normal and abnormal discharges. The solutions that exist in limited current ranges describe patterns, and these patterns seem to represent axially symmetric analogues of the 3D patterns observed in dc glow microdischarges in xenon.

(Some figures in this article are in colour only in the electronic version)

## 1. Introduction

It is well known that current transfer to cathodes of dc glow discharges can occur in the abnormal mode or in the mode with a normal spot, e.g. [1]. This has led to a hypothesis [2] that a self-consistent theoretical model of a near-cathode region in a dc glow discharge must admit multiple steady-state solutions describing different modes of current transfer. In the simplest case where transport of the ions and the electrons in the near-cathode region is dominated by drift, one of these multiple solutions is 1D and describes distributions of parameters that vary along the axis of the discharge but are uniform in the transversal directions. This solution exists at all values of the discharge current and represents an analogue of the well-known solution of von Engel and Steenbeck. The current density–voltage characteristic (CDVC) $U(j)$, described by this solution, is U-shaped, i.e. comprises a falling section and a rising section separated by a point of minimum $j = j_{\min}$. At $j < j_{\min}$ this solution describes the mode associated with the falling section of the CDVC, which is unstable and is not realized. At $j > j_{\min}$ this solution describes the abnormal discharge. The other solutions are multidimensional and their pattern was suggested in [2] on the basis of bifurcation analysis and general trends of self-organization in bistable nonlinear dissipative systems: the modes described by each solution exist in limited ranges of discharge currents, some of these solutions describe patterns with one normal spot and other solutions describe modes with multiple spots.

Two-dimensional simulations based on drift–diffusion equations for the ions and electrons [3–8] revealed only one steady-state solution, which exists at all discharge currents and describes the abnormal discharge at high currents and the normal discharge at lower currents. Clearly, this result does not conform to the above-cited results [2]. Furthermore, while the set of multiple solutions predicted in [2] includes an analogue of the von Engel and Steenbeck solution, the (unique) solution computed in [3–8] is qualitatively different from the von Engel and Steenbeck solution: it predicts the normal mode where the unstable mode associated with the falling section of the CDVC is predicted by the von Engel and Steenbeck solution. These discrepancies are very interesting; however, they apparently have not been discussed.

Recently, the question of multiple solutions in the theory of current transfer to cathodes of dc glow discharges was raised once again in connection with the observations of patterns of more than one spot in dc glow microdischarges [9–13]: these

 

observations were interpreted [14] as an argument in favour of the hypothesis of multiple solutions. However, simulations [15] performed in the framework of the simplest self-consistent model of a glow discharge, which is a discharge between parallel electrodes with a single ion species and transport of the ions and the electrons dominated by drift, without account of complex effects such as a non-local electron energy distribution or the presence of multiple ion and neutral species with a complex chemistry, failed to deliver such solutions. On the other hand, the bifurcation analysis [16] has shown that multiple steady-state solutions must exist even in the framework of this simple model.

In this work, the multiple solutions are computed for the first time. The treatment is limited to axially symmetric solutions. As predicted in [2], the set of solutions includes a solution that exists at all values of the discharge current and solutions that exist in limited current ranges. The mode of current transfer which is described by the former solution and exists at all values of the discharge current will be designated fundamental mode. The nature of this solution depends on whether losses of the ions and electrons due to diffusion to the wall of the discharge vessel are taken into account: if they are not, then this is in essence the von Engel and Steenbeck solution (this is the case considered in [2]); if they are, then this solution describes the abnormal discharge at high currents and the normal discharge at lower currents and is similar to the solutions computed in [3–8]. The solutions that exist in limited current ranges describe patterns, and these patterns seem to represent axially symmetric analogues of the 3D patterns observed in [9–13].

Thus, this work may point the way to a self-consistent description of patterns observed in [9–13] and is in this aspect in line with the recent trend to model self-organization in gas discharges from first principles; see, for example, the modelling of 3D patterns in a dielectric-barrier discharge [17]. (A few further references can be found in [16].)

The outline of the paper is as follows. The model is briefly introduced in section 2. Multiple solutions without diffusion losses are given and discussed in section 3. Also studied in this section are the effect of variation of the tube radius and the role of diffusion of charged particles. The effect over the multiple solutions produced by the diffusion losses is analysed in section 4. Concluding remarks are given in section 5.

## 2. The model

Let us consider a mathematical model of a dc glow discharge comprising equations of conservation of a single ion species and the electrons, transport equations for the ions and the electrons written in the so-called drift–diffusion approximation (i.e. neglecting inertia of the charged particles; e.g. [18]), and the Poisson equation:

$$\nabla \cdot \boldsymbol{J}_\mathrm{i} = n_\mathrm{e}\,\alpha\,\mu_\mathrm{e}\,E - \beta\,n_\mathrm{e}\,n_\mathrm{i},$$

$$\boldsymbol{J}_\mathrm{i} = -D_\mathrm{i}\,\nabla n_\mathrm{i} - n_\mathrm{i}\,\mu_\mathrm{i}\,\nabla\varphi, \tag{1}$$

$$\nabla \cdot \boldsymbol{J}_\mathrm{e} = n_\mathrm{e}\,\alpha\,\mu_\mathrm{e}\,E - \beta\,n_\mathrm{e}\,n_\mathrm{i},$$

$$\boldsymbol{J}_\mathrm{e} = -D_\mathrm{e}\,\nabla n_\mathrm{e} + n_\mathrm{e}\,\mu_\mathrm{e}\,\nabla\varphi, \tag{2}$$

$$\varepsilon_0\,\nabla^2\varphi = -e\,(n_\mathrm{i} - n_\mathrm{e})\,. \tag{3}$$

Here $n_\mathrm{i}$, $n_\mathrm{e}$, $\boldsymbol{J}_\mathrm{i}$, $\boldsymbol{J}_\mathrm{e}$, $D_\mathrm{i}$, $D_\mathrm{e}$, $\mu_\mathrm{i}$ and $\mu_\mathrm{e}$ are number densities, densities of transport fluxes, diffusion coefficients and mobilities of the ions and electrons, respectively; $\alpha$ is Townsend's ionization coefficient; $\beta$ is the coefficient of dissociative recombination; $\varphi$ is the electrostatic potential, $E = |\nabla\varphi|$ is the electric field strength; $\varepsilon_0$ is the permittivity of free space and $e$ is the elementary charge.

Boundary conditions at the cathode and anode are written in the conventional form: diffusion fluxes of the attracted particles are neglected as compared with drift; the normal flux of the electrons emitted by the cathode is related to the flux of incident ions in terms of the effective secondary emission coefficient $\gamma$, which is assumed to characterize all mechanisms of electron emission (due to ion, photon and excited atom bombardment) [1]; density of ions vanishes at the anode; electrostatic potentials of both electrodes are given. One boundary condition at the wall of the discharge vessel is the conventional condition of zero electric current density. Two boundary conditions are used alternatively for $n_\mathrm{i}$ and $n_\mathrm{e}$ at the wall, corresponding to the cases (i) where diffusion losses to the wall are neglected, and (ii) where diffusion losses are taken into account. Let us consider a discharge vessel in the form of a right circular cylinder of a radius $R$ and of a height $h$, and introduce cylindrical coordinates $(r, \phi, z)$ with the origin at the centre of the cathode and the $z$-axis coinciding with the axis of the vessel. Then the boundary conditions read

$$z = 0\colon\ \frac{\partial n_\mathrm{i}}{\partial z} = 0, \qquad J_{\mathrm{e}z} = -\gamma J_{\mathrm{i}z}, \qquad \varphi = 0; \tag{4}$$

$$z = h\colon\ n_\mathrm{i} = 0, \qquad \frac{\partial n_\mathrm{e}}{\partial z} = 0, \qquad \varphi = U; \tag{5}$$

$$r = R\colon\ \begin{array}{ll}\text{(i)} & \dfrac{\partial n_\mathrm{i}}{\partial r} = \dfrac{\partial n_\mathrm{e}}{\partial r} = 0,\\ \text{(ii)} & n_\mathrm{i} = n_\mathrm{e} = 0,\end{array} \qquad J_{\mathrm{i}r} - J_{\mathrm{e}r} = 0. \tag{6}$$

Here $U$ is the discharge voltage, the subscripts $r$ and $z$ denote radial and axial projections of corresponding vectors.

The input parameter for the model can be the discharge voltage $U$ or the discharge current $I$. Both possibilities had to be used in the modelling. To this end, the switching between $U$ and $I$ in the course of calculations has been implemented while building the model. $I$ was used in states where the slope of the current–voltage characteristics (CVC) of the discharge, $U(I)$, is small, in particular, in the vicinity of extreme points of the CVC, on the normal and Townsend discharges. $U$ was used as the input parameter in states where the slope is large, in particular, in the vicinity of turning points and on the subnormal discharge.

It is interesting to note that computation times of models using as input parameters $U$ or $I$ were close, in spite of changes in the structure of the matrix of the system of linear equations in finite elements.

Problem (1)–(6) is well known and represents the most basic self-consistent model of a dc glow discharge. Without account of diffusion losses (i.e. with boundary condition (i) in (6)), the problem admits a 1D solution of the form $f = f(z)$ (here $f$ is any of the quantities $n_\mathrm{i}$, $n_\mathrm{e}$ and $\varphi$), which is in essence the well-known solution of von Engel and Steenbeck [1].

Under certain conditions, the problem admits also 2D (axially symmetric) solutions, $f = f(r, z)$, and 3D solutions, $f = f(r, \phi, z)$. With account of diffusion losses (i.e. with boundary condition (ii) in (6)), the problem admits a 2D solution which was studied in [3–8]. Under certain conditions, the problem admits also other 2D solutions and 3D ones. In this work, multiple 2D solutions are found, both with and without account of diffusion losses.

Numerical results reported in this work have been calculated with the use of a steady-state solver of the commercial finite element software COMSOL Multiphysics. Note that iterative processes in steady-state solvers need not be equivalent to relaxation in time. In particular, the solver being used allows one to decouple questions of numerical and physical stability. For example, one can without any difficulty calculate states on falling branches of CVC treating $U$ as a control parameter, i.e. without a ballast resistance required by solvers based on relaxation in time. Note that this feature is characteristic not only to the COMSOL Multiphysics solver being used but also to other steady-state solvers based on the Newton linearization with a direct solution of linear equations in finite elements or differences, such as the one used in the online tool simulating plasma–cathode interaction in high-pressure arc discharges [19].

The fundamental mode may be found as a matter of routine. However, other solutions are not easy to find: one needs to know in advance what these solutions are like and where they should be sought. This topic will be discussed in some detail in the next sections.

Results reported in this work refer to a discharge in xenon under the pressure of 30 Torr. The interelectrode gap is $h = 0.5$ mm and the radius of the discharge tube $R$ is between 1.5 mm and 0.5 mm. The (only) ionic species considered is $Xe_2^+$. The mobility of $Xe_2^+$ ions in Xe was evaluated by means of the formula $\mu_i = 2.1 \times 10^{21}\,\mathrm{m^{-1}\,V^{-1}\,s^{-1}}/n_n$ (here $n_n$ is the density of the neutral gas), which is an approximation of the measurements [20]. The mobility of the electrons was evaluated as $\mu_e = 17\,\mathrm{Torr\,m^2\,V^{-1}\,s^{-1}}/p$, where $p$ is the pressure of the plasma; Townsend's ionization coefficient $\alpha$ was evaluated as $\alpha = Cp\exp[-D(p/E)^{1/2}]$ with $C = 6.53 \times 10^3\,\mathrm{m^{-1}\,Torr^{-1}}$ and $D = 3.61 \times 10^2\,\mathrm{V^{1/2}(m\,Torr)^{-1/2}}$ [1]. (Note that this way of evaluation of $\mu_e$ and $\alpha$ yields results in good agreement with those given by the zero-dimensional Boltzmann solver BOLSIG+ [21].) The diffusion coefficients were evaluated by means of Einstein's law, $D_{i,e} = k\,T_{i,e}\,\mu_{i,e}/e$, where $k$ is Boltzmann's constant and $T_i$ and $T_e$ are temperatures of the heavy particles and electrons, respectively; $T_i = 300$ K and $T_e = 1$ eV. The coefficient of dissociative recombination of molecular ions $Xe_2^+$ was set equal to $2 \times 10^{-13}\,\mathrm{m^3\,s^{-1}}$ [22, 23]. The effective secondary emission coefficient was set equal to 0.03.

## 3. Solutions without diffusion losses

In this section, 2D solutions without account of diffusion losses are considered, i.e. with boundary condition (i) in (6). Information on what these solutions are like and where they should be sought was obtained by means of finding bifurcation points where 2D modes branch off from the fundamental (1D) mode. Calculation of each 2D mode was started in the vicinity of the corresponding bifurcation point with an initial approximation obtained by adding to the 1D solution a small radial perturbation governed by a Bessel function [24]. When a state belonging to the desired 2D mode has been found, the next step is to vary the input parameter ($U$ or $I$) in order to find the 2D mode in the whole range of its existence.

The 1D eigenvalue problem governing the location of bifurcation points in the framework of the present model is similar to the one considered in [16], except that the diffusion terms are taken into account in the transport equations for the ions and the electrons in this work.

### 3.1. Multiple solutions

Results reported in this section refer to a discharge tube of the radius $R = 1.5$ mm. Multiple solutions describing nine different modes were detected in this case, a 1D mode and eight 2D modes. The CVCs of the 1D mode and five 2D modes are shown in figure 1. Here $\langle j \rangle$ is the average value of the axial component of the electric current density evaluated over the whole surface of the cathode or, equivalently, over a whole (circular) cross section of the discharge vessel. The 1D mode exists at all values of the discharge current and is termed fundamental mode; this is an analogue of the well-known solution of von Engel and Steenbeck [1]. Each of the 2D modes exists in a limited range of the discharge current and its CVC represents a closed curve. For each of the 2D modes, there are two states in which functions $n_i$, $n_e$ and $\varphi$ vary with $z$ but not with $r$, i.e. $n_{i,e} = n_{i,e}(z)$ and $\varphi = \varphi(z)$. These states are marked by circles in figure 1 and subsequent figures. One of these two states is close to the point of minimum of the CVC of the fundamental mode and is designated $a_i$ ($i = 1, 2, \ldots, 8$), the other is designated $b_i$ and located at lower currents. These states belong not only to the 2D mode being considered but also to the fundamental mode. In other words, the solutions describing the 2D mode and the fundamental mode coincide at these states. This phenomenon is well known in mathematical physics and called bifurcation, or branching, of solutions, and states where it occurs are called bifurcation points.

The point of minimum of the CVC of the fundamental mode, found by means of the 2D simulations, is $j_{min} \approx 325\,\mathrm{A\,m^{-2}}$. The two nearest bifurcation points determined in the above-described way (i.e. as states belonging to 2D modes where distributions of parameters become 1D) are located at $j \approx 329\,\mathrm{A\,m^{-2}}$ and $j \approx 325\,\mathrm{A\,m^{-2}}$. One could think that the first bifurcation point is positioned on the section of the fundamental mode with a rising CVC. However, the numerical accuracy of the 2D modelling is insufficient to judge. An alternative way of finding bifurcation points is to solve the 1D eigenvalue problem mentioned at the beginning of section 3. The bifurcation points determined in this way which are the nearest to the point of minimum of the CVC of the fundamental mode are located at $j = 327\,\mathrm{A\,m^{-2}}$ and $j = 322\,\mathrm{A\,m^{-2}}$ and the point of minimum found by means of 1D simulations is $j_{min} = 328\,\mathrm{A\,m^{-2}}$. These values are accurate and one can see that the bifurcation points are positioned on the section of

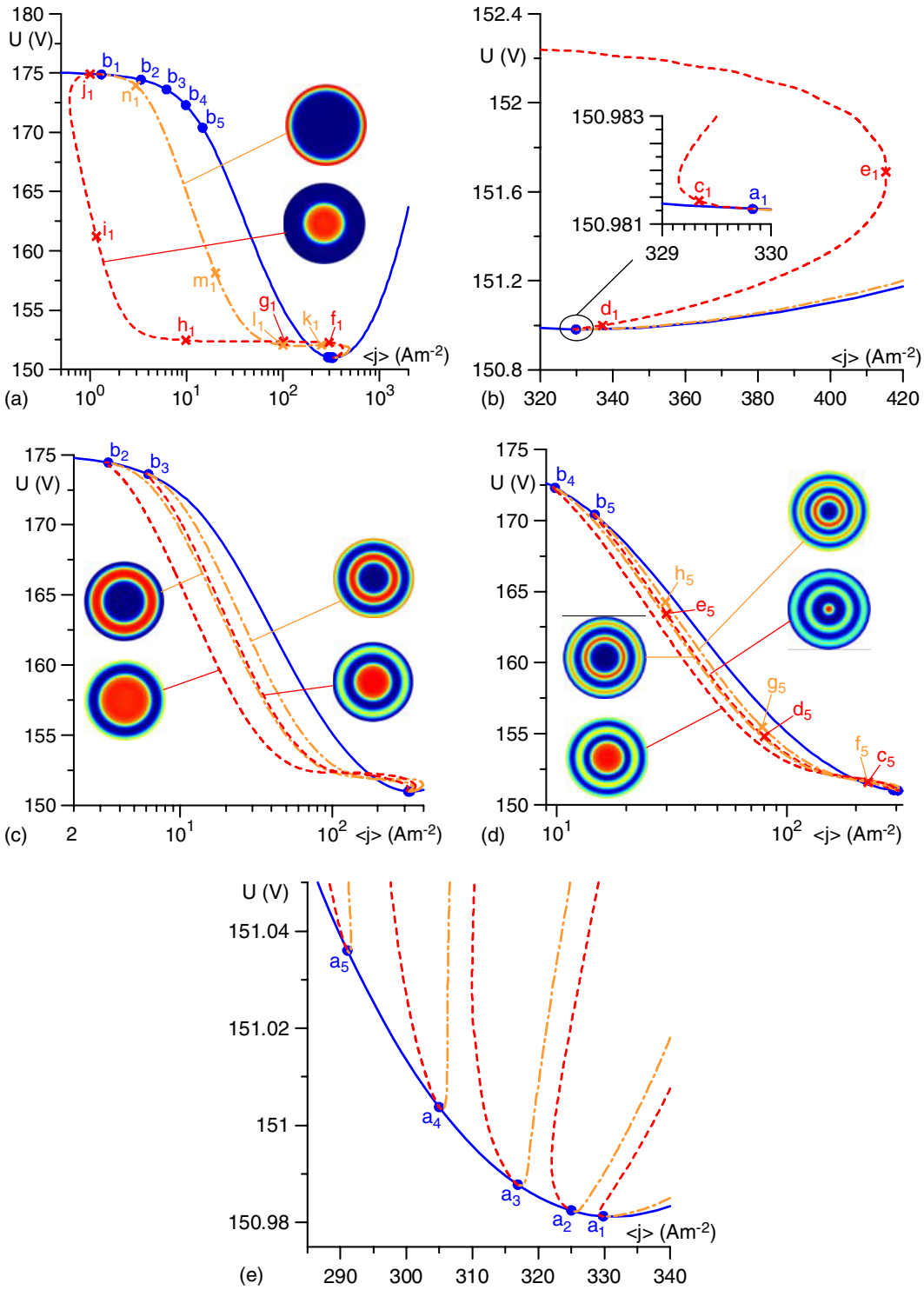


**Figure 1.** CVCs. $R = 1.5$ mm, diffusion losses neglected. Solid: the fundamental mode. Dashed: branches of 2D modes associated with patterns comprising a spot at the centre of the cathode. Dashed–dotted: branches of 2D modes associated with patterns without a central spot. (*a*) The first 2D mode and the fundamental mode; (*b*) details of the CVC of the first 2D mode near the bifurcation point $a_1$; (*c*) the second and third 2D modes and the fundamental mode; (*d*) the fourth and fifth 2D modes and the fundamental mode; (*e*) details of the CVCs near the minimum of the CVC of the fundamental mode.

the fundamental mode with a falling CVC, which is a usual situation.

Let us designate by $I(a_i)$ and $I(b_i)$ values of the discharge current that correspond to bifurcation points $a_i$ or, respectively, $b_i$. We number the bifurcation points such that $I(b_1) < I(b_2) < \cdots < I(b_8) < I(a_8) < I(a_7) < \cdots < I(a_1)$. Analysis of figure 1 with necessary magnifications reveals that the 2D mode that bifurcates at $a_1$ is the same that bifurcates at $b_1$. In the following, this mode will be referred to as the first 2D mode. Similarly, the 2D mode that bifurcates at $a_2$ is the same that bifurcates at $b_2$; the second 2D mode, etc.

The (two) bifurcation points positioned on each 2D mode divide this mode into two branches. Schematics in figure 1 illustrate current density distributions over the cathode surface corresponding to each branch. One of the branches of the first 2D mode is associated with a pattern comprising a spot at the centre of the cathode, the other branch is associated with a pattern comprising a ring spot at the periphery. One of the branches of the second 2D mode is associated with a pattern comprising a spot at the centre and a ring spot at the periphery, the other branch with a pattern comprising a ring spot in the interior of the cathode. One of the branches of the third 2D mode is associated with patterns comprising a spot at the centre and an interior ring spot, the other with an interior ring spot and a spot at the periphery. One of the branches of the fourth 2D mode is associated with patterns comprising a spot at the centre, an interior ring spot and a spot at the periphery, the other with two interior ring spots. One of the branches of the fifth 2D mode is associated with patterns comprising a spot at the centre and two interior ring spots, the other with two interior ring spots and a spot at the periphery. Generalizing, one can say that one of the two branches of each 2D mode is associated with a pattern comprising a spot at the centre of the cathode and the other with a pattern without a central spot.

In the vicinity of each bifurcation point, e.g. the point $a_i$, the bifurcating 2D mode exists at currents both below and above $I(a_i)$. (This can be seen from figure 1($b$) as far as the point $a_1$ is concerned, from figure 1($e$) as far as the points $a_2$, $a_3$, $a_4$, $a_5$ are concerned from figure 1($a$) as far as the point $b_1$ is concerned and from appropriate magnifications of the vicinities of points $b_2$, $b_3$, $b_4$, $b_5$ in figures 1($c$) and ($d$).) In other words, if a branch of an $i$th 2D mode bifurcates into the current range $I < I(a_\mathrm{i})$, then the other branch of the same mode bifurcates into the range $I > I(a_\mathrm{i})$. Furthermore, it can be seen that the branch of an $i$th mode associated with a pattern comprising a spot at the centre bifurcates into the range $I < I(a_i)$ in the vicinity of the bifurcation point $a_i$ and into the range $I < I(b_i)$ in the vicinity of the bifurcation point $b_i$, while the branch associated with a pattern without a central spot bifurcates into the ranges $I > I(a_i)$ and $I > I(b_i)$.

According to the bifurcation theory [16], a solution describing an $i$th 2D mode in the vicinity of both bifurcation points $a_\mathrm{i}$ and $b_\mathrm{i}$ represents a superposition of a 1D solution and a small 2D perturbation with the radial variation governed by the Bessel function of the first kind of order zero, $J_0(k\,r)$, where $k = 3.832/R$, $k = 7.016/R$, $k = 10.17/R$, $k = 13.32/R$ and $k = 16.47/R$ for the first, second, third, fourth and fifth 2D modes, respectively. (Note that numbers 3.832, 7.016, 10.17, 13.32 and 16.47 represent abscissas of the first five extrema of the function $J_0(x)$.) This variation is indeed seen in the numerical results.

The complexity of the patterns associated with the 2D modes increases with $i$ or, equivalently, with a decrease in the range of existence of the corresponding mode. This is a behaviour typical for bistable nonlinear dissipative systems. Note that the two stable regimes of the glow discharge are represented by the 1D abnormal discharge and the case where the discharge has not been ignited [14].

Variations of a pattern associated with a given branch from one bifurcation point to the other are illustrated by figure 2. Figures 2($a$) and ($b$) show variations of the pattern with a central spot, associated with one of the branches of the first 2D mode. In the state $a_1$, which is a bifurcation point, the current density is the same at all points of the cathode surface. A weak variation of the current density over the cathode surface occurs in the vicinity of the bifurcation point (state $c_1$) and this variation is well described by the Bessel function $J_0(3.832\,r/R)$. Further away from the bifurcation point $a_1$ (state $d_1$), the current density at the cathode surface increases, except in the vicinity of the wall where it decreases. One can say that a current spot is being formed that occupies the whole surface of the cathode except the vicinity of the wall. The state $e_1$ represents a turning point of the branch being considered. The formation of the spot has already finished and the spot starts shrinking. At states $f_1$ and $g_1$ the spot continues to shrink, while the current density inside the spot does not change much. From state $h_1$ the spot stops shrinking and the maximum current density inside the spot starts decreasing. There is still a well pronounced spot in state $i_1$. Further on, the spot becomes less pronounced. In the vicinity of the bifurcation point $b_1$ (state $j_1$), there is again only a weak variation of the current density along the cathode surface which is well described by the Bessel function $J_0(3.832\,r/R)$. The current density becomes constant along the cathode surface at the bifurcation point $b_1$. Note that the above-described numerical results conform to the analytical theory [25] as they should.

The above-described approximate constancy of current density inside the spot between states $e_1$ and $h_1$ is associated with the plateau of the CVC represented in figure 1($a$). These features are characteristic of the effect of normal current density. Hence, the section of the central-spot branch of the first 2D mode corresponding to the plateau of the CVC may be identified with the normal mode of the glow discharge.

Values of the current density inside the normal spot considerably exceed the current density at the minimum of the CVC of the fundamental mode, $j_\mathrm{min} \approx 325\,\mathrm{A\,m^{-2}}$, in contrast to what is sometimes believed. Rather, the current density inside the normal spot approximately corresponds to the current density which occurs on the abnormal mode at the same discharge voltage. For example, the value of discharge voltage in state $f_1$ is $U = 152.26\,\mathrm{V}$. At this $U$, the current density in the abnormal mode equals $610\,\mathrm{A\,m^{-2}}$, which is quite close to the maximum value of current density in state $f_1$, equal to $599\,\mathrm{A\,m^{-2}}$. Similarly, $U = 152.36\,\mathrm{V}$ in state $g_1$; the current density at this $U$ in the abnormal mode equals $624\,\mathrm{A\,m^{-2}}$ and is quite close to the maximum value of current density in state $g_1$, which is $632\,\mathrm{A\,m^{-2}}$. Hence, one can view the effect of normal current density as a manifestation of coexistence of a hot phase, representing the abnormal mode, with a cold phase, representing a situation in which no discharge is present at the considered point of the cathode surface [25]. Note that the concept of coexistence of phases gives a hint as to why the discharge voltage is virtually constant in the normal mode: the coexistence of phases is usually possible at only one value of the control parameter, in this case, $U$. (This value is governed by a certain condition which follows from a treatment of an intermediate region that separates the phases and is known as Maxwell's construction; see, e.g. [26].)

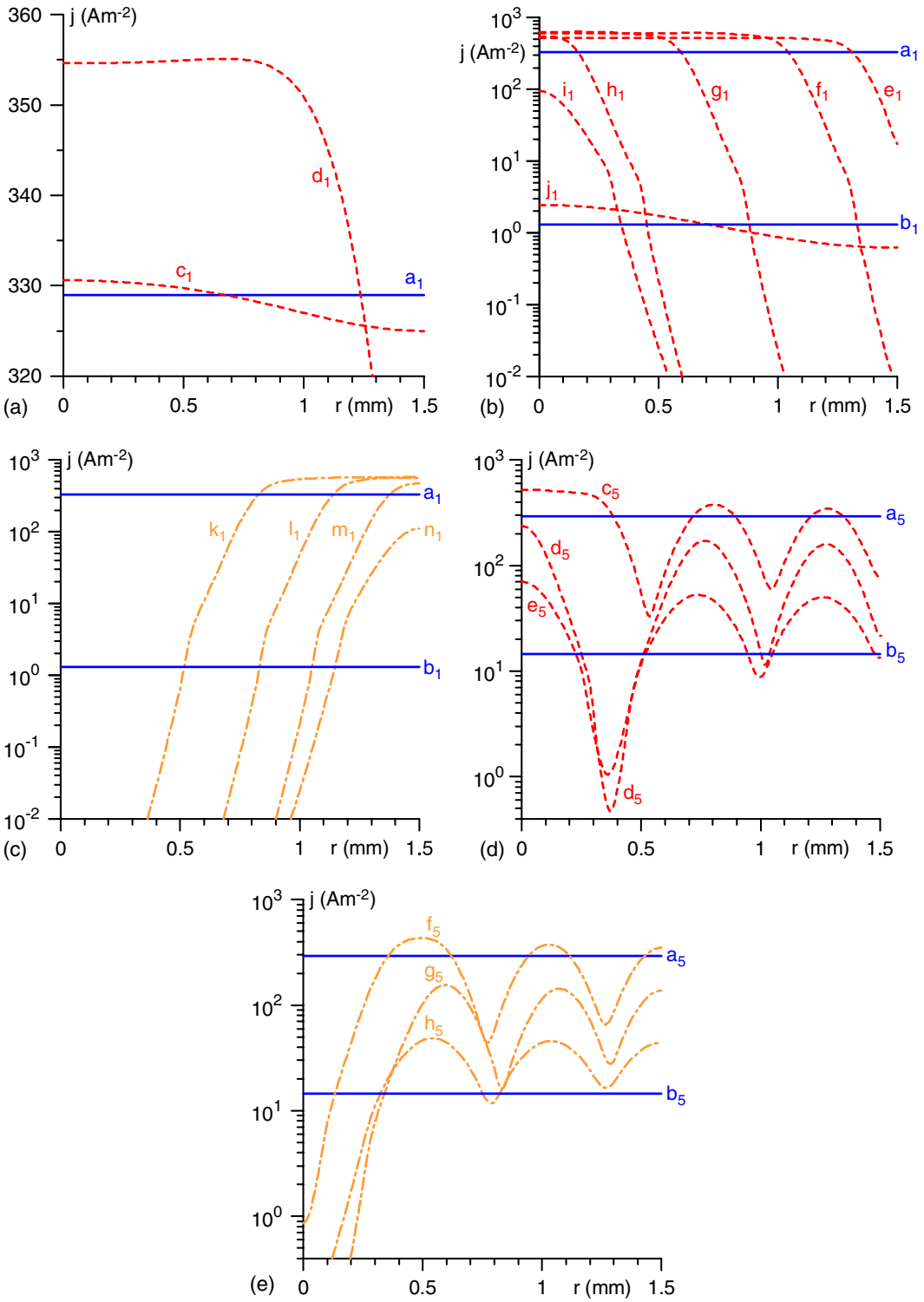


**Figure 2.** Distributions of current density over the cathode surface for the first and fifth 2D modes. $R = 1.5$ mm, diffusion losses neglected. (*a*), (*b*) The branch with a spot at the centre of the cathode; (*c*) the branch with a ring spot at the periphery of the cathode; (*d*) the branch with a spot at the centre of the cathode and two interior ring spots; (*e*) the branch with two interior ring spots and a ring spot at the periphery of the cathode. The states to which each of the lines correspond are indicated in figures 1(*a*), (*b*), (*d*) and (*e*).

A plateau is also present on the CVC of the branch of the first 2D mode associated with the ring spot on the periphery, as can be seen in figure 1(*a*). The maximum of current density inside the spot between states $k_1$ and $l_1$ remains more or less constant, as is seen in figure 2(*c*). The value of the discharge voltage $U$ in state $k_1$ is 152.04 V and the value of the current density corresponding to this $U$ in the abnormal mode is 566 A m$^{-2}$, which exactly coincides with the maximum of current density in state $k_1$. For state $l_1$, $U$ is 152.05 V. The value of the current density in the abnormal mode corresponding to this $U$ is 576 A m$^{-2}$, approximately equal to the maximum of current density in state $l_1$ which

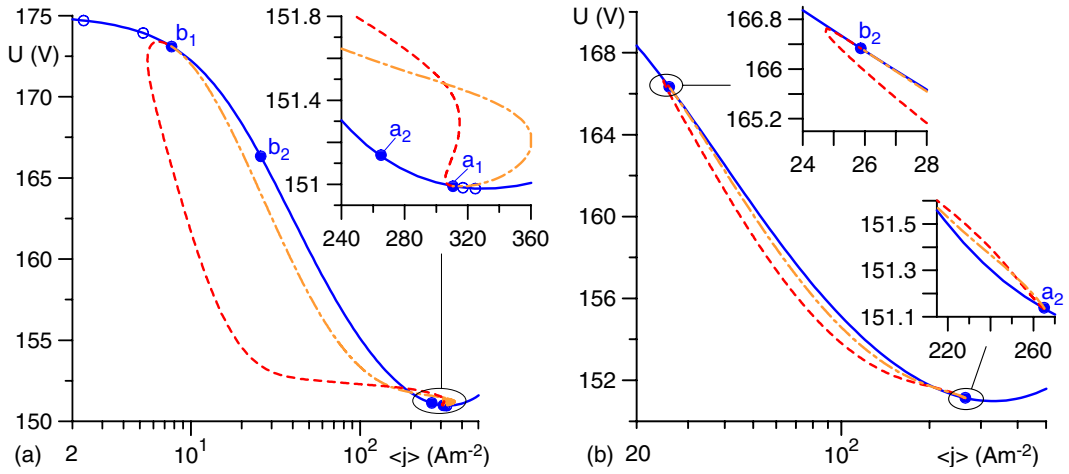


**Figure 3.** CVCs. $R = 0.5$ mm, diffusion losses neglected. Solid: the fundamental mode. Dashed: branches of 2D modes associated with patterns comprising a spot at the centre of the cathode. Dashed–dotted: branches of 2D modes associated with patterns without a central spot. (*a*) The first 2D mode and fundamental mode; (*b*) the second 2D mode and the fundamental mode.

is 570 A m$^{-2}$. One can conclude that the effect of normal current density is also present on the branch of the first 2D mode associated with the ring spot on the periphery, although it occurs in a current range substantially more narrow than on the branch with the central spot.

The effect of normal current density is manifested also by the second and subsequent 2D modes; however, with increasing $i$ it becomes less pronounced and occurs in a narrower range of the discharge currents and eventually disappears. The only feature of the fifth 2D mode (figures 2(*d*) and (*e*)) that reminds of this effect is a more or less constant current density inside the central spot in state $c_5$.

### 3.2. The effect of variation of the radius

Calculations for a discharge tube of the radius $R = 0.5$ mm revealed only two 2D modes; see figure 3. Also shown in this figure is the fundamental mode (which is the same as the one found for $R = 1.5$ mm). Average current densities corresponding to the bifurcation points positioned on the first and second 2D modes are $\langle j(a_1)\rangle = 311$ A m$^{-2}$, $\langle j(b_1)\rangle = 7.7$ A m$^{-2}$, $\langle j(a_2)\rangle = 265$ A m$^{-2}$ and $\langle j(b_2)\rangle = 26$ A m$^{-2}$. Note that the similar values for $R = 1.5$ mm are $\langle j(a_1)\rangle = 329$ A m$^{-2}$, $\langle j(b_1)\rangle = 1.3$ A m$^{-2}$, $\langle j(a_2)\rangle = 325$ A m$^{-2}$ and $\langle j(b_2)\rangle = 3.4$ A m$^{-2}$. One can conclude that a decrease in $R$ causes a shift of the two bifurcation points belonging to each 2D mode in the directions towards each other. The range of existence of each of the 2D modes also shrinks with a decrease in $R$.

Calculations for intermediate $R$ have shown that the third to eighth 2D modes disappear one by one with decreasing $R$, and the disappearance occurs through shrinking of their existence ranges. As an example, the disappearance of the third 2D spot mode is shown in figure 4 in the plane $(j_c, \langle j\rangle)$. (Here $j_c$ is the current density at the centre of the cathode; these coordinates have been chosen since the CVCs for the different values of $R$ shown in figure 4 are nearly coincident.) As $R$ decreases, the bifurcation points $a_3$ and $b_3$ move towards each other. There is only one bifurcation

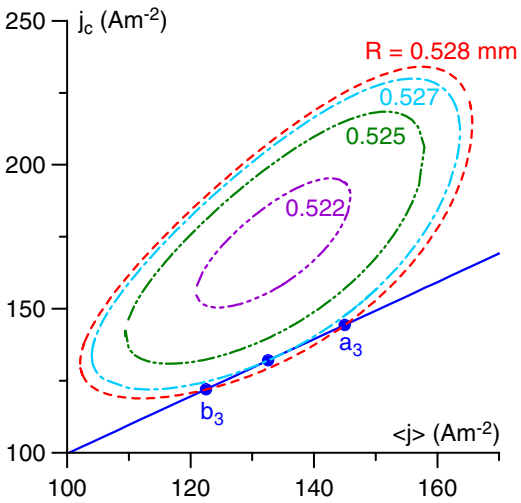


**Figure 4.** Electric current density at the centre of the cathode versus average current density for the third 2D mode for discharge tubes of different radii. Diffusion losses neglected.

point at $R \approx 0.527$ mm. At $R \lesssim 0.527$ mm, the 2D spot mode is detached from the diffuse mode and its existence range continues to shrink. It is interesting to note that all states of the third 2D mode at $R \lesssim 0.527$ mm possess a spot at the centre of the cathode and an interior ring spot. No steady states belonging to the third 2D mode have been found at $R \lesssim 0.520$ mm.

A more or less pronounced effect of normal current density is present at $R = 0.5$ mm only on the first 2D mode, as evidenced by the CVCs shown in figure 3.

### 3.3. The role of diffusion of the charged particles

An interesting question is to what extent the above results are affected by diffusion of the charged particles. Results of calculation of the fundamental mode and the first 2D mode with the ion and electron diffusion coefficients reduced by a factor of two or four (or, equivalently, with the ion and electron

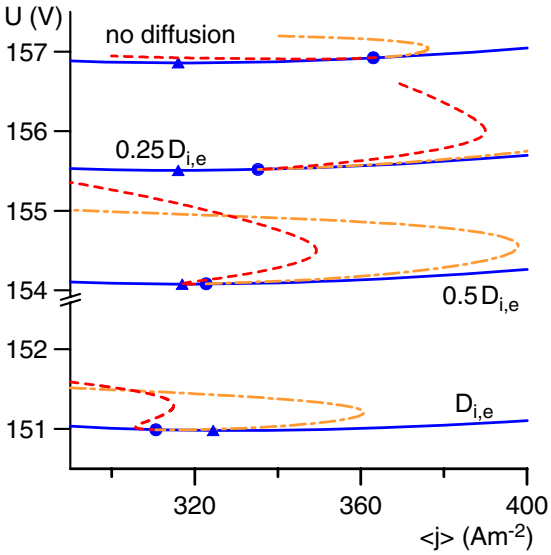


**Figure 5.** CVCs of the fundamental mode and of the first 2D mode for different diffusion coefficients near the minimum of the CVC of the fundamental mode. $R = 0.5$ mm, diffusion losses to the wall neglected. Solid: the fundamental mode. Dashed: branch with a spot at the centre of the cathode. Dashed–dotted: branch with a ring spot at the periphery of the cathode.

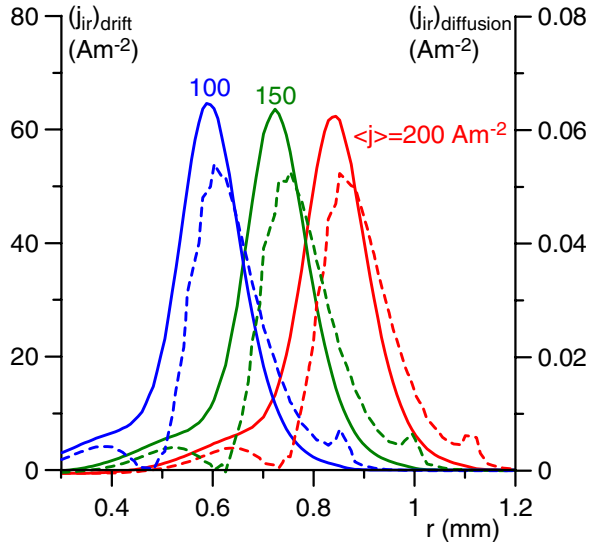


**Figure 6.** Distribution of components of radial projection of the ion current density in the cross section $z = 0.06$ mm. The first 2D mode, $R = 1.5$ mm, $z = 0.06$ mm, diffusion losses to the wall neglected. Solid: drift component. Dashed: diffusion component.

temperatures reduced by a factor of two or four) in the vicinity of the minimum of the CVC of the fundamental mode are shown in figure 5. Also shown are results of calculations with the original values of $D_i$ and $D_e$, as well as results of calculations without account of diffusion. The bifurcation points are represented by circles and the points of minimum of the CVC of the fundamental mode by triangles. The branch of the 2D mode associated with a spot at the centre of the cathode in all the cases branches off into the range of low currents, although this can hardly be seen on the graph or cannot be seen at all. Note that the 2D mode in the case where the diffusion is neglected could only be calculated in the vicinity of the bifurcation point: the upper curve in figure 5 represents all the states where converged solutions have been obtained. (The width of this vicinity strongly depends on the numerical mesh; the results depicted in figure 5 have been calculated with the use of a non-uniform mesh with 18 500 degrees of freedom.) The position of the bifurcation point in the case without diffusion conforms to the numerical accuracy to the one found in [16], as it should.

As the diffusion coefficients are reduced, the discharge voltage slightly increases. (As far as the fundamental mode is concerned, it is already known that neglect of diffusion causes a weak increase in the discharge voltage not only in the vicinity of the minimum of its CVC but at all currents [24].) Two turning points visible on the branch of the 2D mode associated with a spot at the centre in the cases of the original and reduced diffusion coefficients disappear in the cases without diffusion. As the diffusion coefficients are reduced, the bifurcation point is shifted in the direction of higher currents and eventually crosses the point of minimum of the CVC of the fundamental mode and enters the rising section of the CVC. Thus, the present modelling confirms the conclusion [16] on the possibility of a bifurcation on a discharge mode with a positive differential resistance, a result very interesting theoretically.

One can conclude that the overall effect of diffusion is visible, but not very strong.

In figure 6, distributions of drift and diffusion components of radial projection of the ion current density in the cross section of the discharge at 0.06 mm from the cathode are shown for several states belonging to the normal discharge. The cross section $z = 0.06$ mm approximately corresponds to the point of maximum of the distribution of the density of space charge along the axis of the discharge and is positioned more or less in the middle of the cathodic space-charge sheath. Note that the maxima of both drift and diffusion currents are located at the edge of the spot, as could be expected.

One can see from figure 6 that the drift current exceeds the diffusion current by three orders of magnitude. On the other hand, the diffusion still plays an important role, since the 2D mode without account of diffusion could only be calculated in the vicinity of the bifurcation point as mentioned above.

The question of the effect of diffusion of charged particles over the structure of normal spots is very interesting and has been raised in the literature more than once; e.g. [4, 25]. Leaving a detailed analysis beyond the scope of this work, we only note that a hypothetical explanation of the above results may be offered on the basis of analogy with the problem of calculation of shock waves in gas dynamics. It is well known that if dissipative processes are neglected, then shock waves appear (in the framework of the Euler equations) as discontinuities; if dissipative processes are taken into account, then shock waves may be resolved (in the framework of the Navier-Stokes equations). Similarly, one can hypothesize that the spot patterns in principle may appear without diffusion, due only to electrostatic effects and drift, however far away from the bifurcation points such patterns manifest abrupt transitions from spots to the surrounding current-free region and are

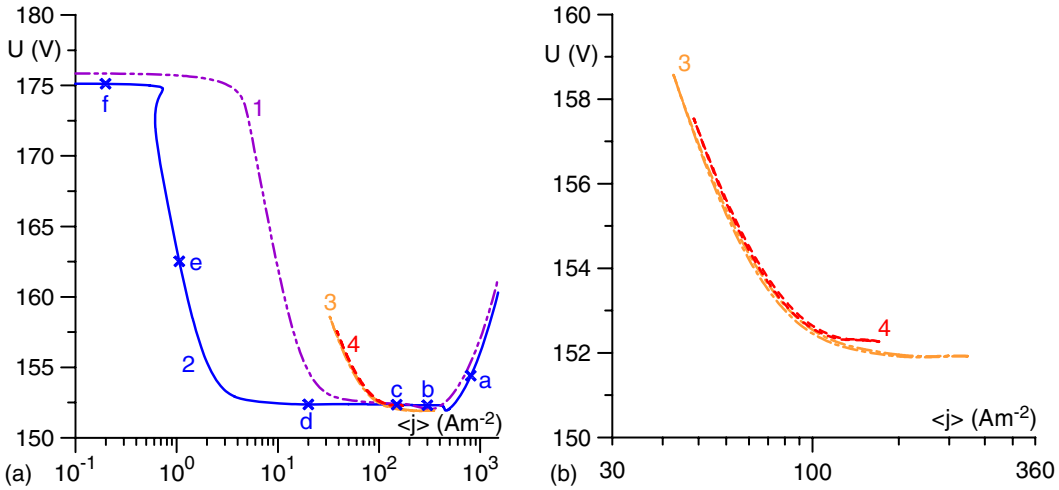


**Figure 7.** CVCs. Diffusion losses taken into account. 1: Fundamental mode, $R = 0.5$ mm. 2: Fundamental mode, $R = 1.5$ mm. 3: The first non-fundamental 2D mode, $R = 1.5$ mm. 4: The second non-fundamental 2D mode, $R = 1.5$ mm. (*a*) General view; (*b*) magnification of the first and second non-fundamental 2D modes.

described by discontinuous solutions, which are difficult to calculate.

## 4. Solutions with diffusion losses

When diffusion losses to the wall are taken into account, the fundamental mode is no longer 1D but rather becomes 2D. Furthermore, the non-fundamental 2D modes do not bifurcate from the fundamental mode. Under these circumstances it is not possible to rely on bifurcation analysis in order to obtain information on the range of existence of non-fundamental 2D modes or what these modes are like.

The procedure of finding these modes was as follows. Starting from a state belonging to a 2D mode without diffusion losses, the diffusion losses are gradually introduced for a fixed value of the input parameter (the discharge voltage or current). Note that the transition between states with and without diffusion losses is non-trivial and is described in detail elsewhere [24].

Three 2D modes have been found for $R = 1.5$ mm. One of them exists at all current values, i.e. is fundamental, the other two modes exist only in limited current ranges. The CVCs of the three modes are shown in figure 7(*a*). The CVCs of the two non-fundamental 2D modes are also shown in figure 7(*b*). The modes are all disconnected from each other, although CVCs intersect at some values of the discharge current. The CVCs of the non-fundamental modes represent closed curves and each mode is constituted by two branches separated by two turning points. The difference between values of the discharge voltage on different branches for the same value of $\langle j \rangle$ amounts to a few tens of millivolts and thus is hardly visible even in figure 7(*b*). Also shown in figure 7(*a*) is the fundamental mode for $R = 0.5$ mm. No other 2D modes have been found for this value of $R$.

Distributions of current density over the cathode surface at several states belonging to the fundamental mode for $R = 1.5$ mm are shown in figure 8. The current density in state *a* is constant over the most part of the cathode surface

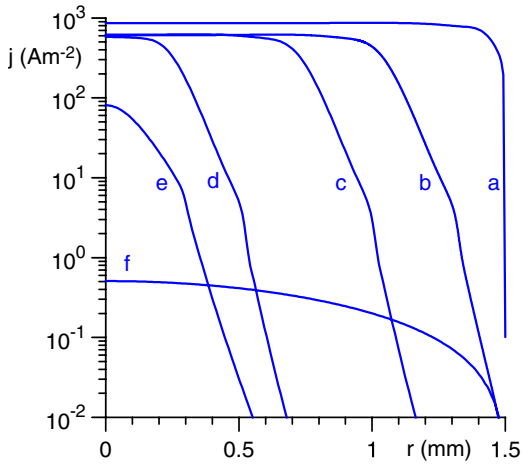


**Figure 8.** Distributions of current density over the cathode for the fundamental mode. $R = 1.5$ mm, diffusion losses taken into account. The states to which each of the lines correspond are indicated in figure 7.

and sharply drops in the immediate vicinity of the wall. This distribution may be identified with the abnormal discharge. As the discharge current decreases, a normal spot at the centre of the cathode appears (states *b*, *c*, *d*). Somewhere between states *d* and *e* the spot stops shrinking and the maximum current density inside the spot starts decreasing; the subnormal discharge. Somewhere between states *e* and *f* the spot starts expanding, while the current density inside the spot continues to decrease. Eventually the Townsend discharge is formed with the radial dependence of current density described by the Bessel function $J_0(2.42\, r/R)$, in agreement with the theory [6] (state *f*).

In figure 9 maxima of numerically calculated distributions of the densities of charged particles along the axis of the discharge are shown as functions of $\langle j \rangle$. Also shown are analytical results for the limiting case of the Townsend discharge obtained along the lines [6]. (Note that these results are independent of the radius of the tube.) One can see

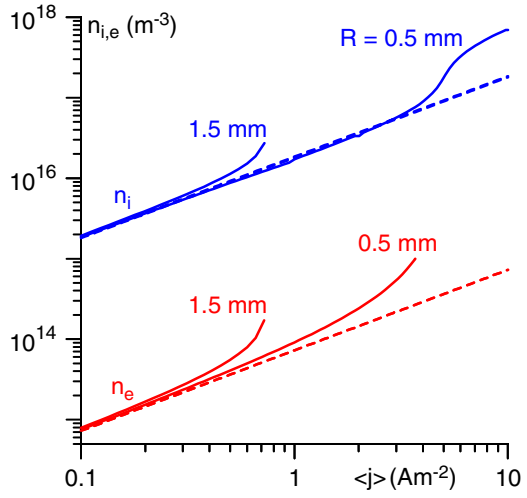


**Figure 9.** Maxima of densities of charged particles on the axis of the discharge. Diffusion losses taken into account. Solid: numerical results. Dashed: analytical results for the limiting case of the Townsend discharge.

that the Townsend discharge occurs at $\langle j \rangle$ of the order of or below 1 A m$^{-2}$, in agreement with what can be concluded from figure 7(*a*).

Thus, the fundamental solution describes the abnormal discharge, the normal discharge, the subnormal discharge and the Townsend discharge, and is similar to the solutions computed in [3–8].

The value of the discharge voltage $U$ in state *b* is 152.32 V. At this $U$, the current density on the rising section of the CVC of the fundamental mode without diffusion losses is 610 A m$^{-2}$, which exactly coincides with the maximum value of the current density over the cathode surface in state *b*. Similarly, $U = 152.34$ V in state *c*; the current density at this $U$ on the rising section of the CVC of the fundamental mode without diffusion losses is 614 A m$^{-2}$ and is quite close to the maximum value of the current density over the cathode surface in state *c*, which equals 624 A m$^{-2}$. Hence, the effect of normal current density in the glow discharge with diffusion losses can still be interpreted as a manifestation of coexistence of phases, provided that the hot phase is understood as the 1D abnormal discharge, i.e. the abnormal discharge without diffusion losses.

The ratio of the numerically computed electron current to the wall of the discharge tube to the discharge current is of the order of $10^{-3}$ or lower at all discharge currents. In other words, diffusion of the charged particles to the wall represents a weak effect. It is not surprising therefore that the distribution of current density over the cathode surface in states on the abnormal mode is virtually uniform except in a thin layer near the wall of the vessel, as shown by line a in figure 8. On the other hand, the Townsend discharge manifests a radial variation governed by the Bessel function as shown by line f in figure 8, i.e. is essentially non-uniform. A question arises as to how diffusion of the charged particles to the wall, which is a weak effect, can affect the discharge that significantly. Note that this question seems to have been discussed for the first time in the work [7].

The root cause of this effect is the linearity of process of multiplication of the charged particles in the Townsend discharge. Consider an initial situation where a uniform flux of electrons is emitted from the cathode surface. Each electron produces on average $1/\gamma$ ions while travelling to the anode. The ions return to the cathode and are converted into one electron, and this completes the cycle. However, a part of the ions and the electrons produced inside a layer adjacent to the wall, as well as a part of the electrons emitted into this layer, will diffuse to the wall and will be absorbed there. A scale of thickness of this layer may be estimated as $L = v_{\rm dif}\tau$, where $\tau = h^2/\mu_e U$ is a characteristic time of drift of electrons from the cathode to the anode and $v_{\rm dif} = D_e/R$ is a characteristic velocity of free diffusion of electrons to the wall of the vessel. One finds that $L$ is of the order of $10^{-3}$ mm, i.e. much smaller than both $h$ and $R$, in accordance with the above conclusion on smallness of the diffusion losses.

Thus, a near-wall layer of a thickness of the order $L$ is depleted of charged particles after the first cycle. After the second cycle, the thickness of the depleted layer will double, etc. The Bessel radial dependence in $n_i$ and $n_e$ appears after many cycles.

The distributions of current density over the cathode surface for several states belonging to the non-fundamental 2D modes and corresponding to different values of the discharge current are shown in figure 10. Both branches of the first non-fundamental 2D mode are associated with a ring spot inside the cathode, both branches of the second non-fundamental 2D mode are associated with a pattern comprising a spot at the centre of the cathode and an interior ring spot. Distributions of parameters in states belonging to different branches of the same mode and corresponding to the same discharge current are surprisingly close.

An example of distribution of parameters in the interelectrode gap is shown in figure 11. Arrows in figure 11(*c*) indicate local directions of the electric current and their length is proportional to the modulus of current density.

Two current filaments are seen, one in the form of a cylinder at the centre of the cathode and the other, which is not very well pronounced, in the form of a toroid. These filaments correspond to the central and, respectively, ring current spots on the cathode seen in figure 10(*b*). The distribution of parameters inside the central part of the cylindrical filament is close to 1D. The densities of the charged particles and modulus of the current density drop by at least two orders of magnitude in the space between the filaments, the electric field here is more uniform. This picture again can be interpreted as the coexistence of hot and cold phases.

## 5. Concluding remarks

Multiple steady-state solutions in the theory of dc glow discharge have been found for the first time. The modelling is performed in 2D in the framework of the simplest self-consistent model of glow discharge, comprising equations of conservation of a single ion species and the electrons, transport equations for the ions and the electrons written in the drift–diffusion approximation and the Poisson equation.

When losses of the ions and the electrons due to diffusion to the wall are neglected, solutions describing nine different

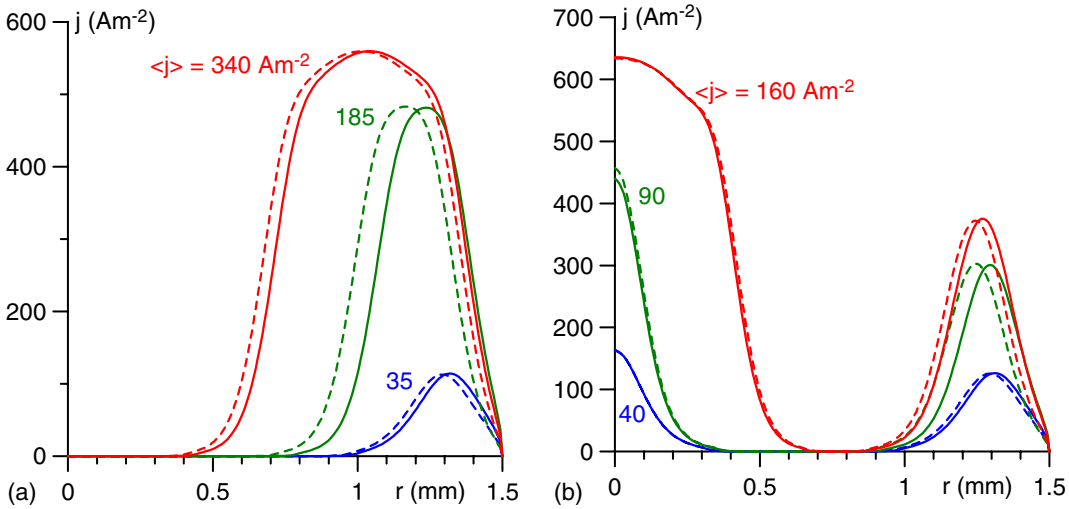


**Figure 10.** Distributions of current density over the cathode for the first (*a*) and second (*b*) non-fundamental 2D modes. $R = 1.5$ mm, diffusion losses taken into account. Solid/dashed: distributions corresponding to the branch with a lower/higher voltage.

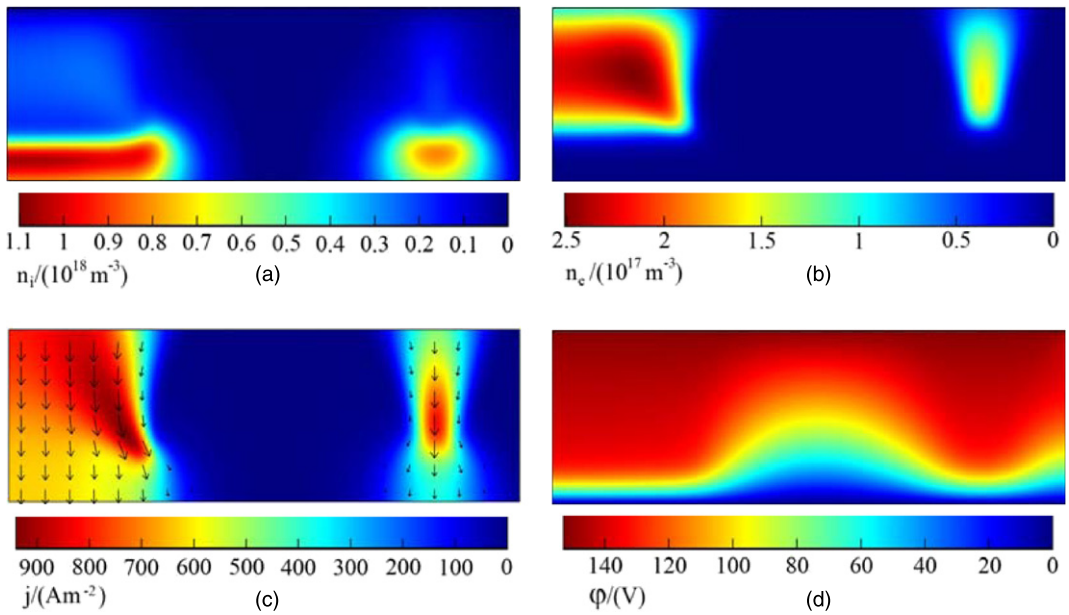


**Figure 11.** Distributions of parameters in the interelectrode gap. The second non-fundamental 2D mode, $\langle j \rangle = 170\ \mathrm{A\,m^{-2}}$, $R = 1.5$ mm, diffusion losses taken into account. (*a*) $n_\mathrm{i}$, (*b*) $n_\mathrm{e}$, (*c*) modulus of current density, (*d*) $\varphi$. Bottom: cathode, top: anode; left: axis of symmetry; right: wall of the discharge vessel.

modes were detected in the case of a discharge tube of the radius $R = 1.5$ mm. One mode is 1D, is fundamental (i.e. exists at all values of the discharge current) and represents in essence the well-known solution of von Engel and Steenbeck. The other eight modes are 2D (axially symmetric) and exist in limited ranges of the discharge currents. Each 2D mode is constituted by two branches, one associated with a pattern comprising a spot at the centre of the cathode and the other with a pattern without a central spot. The branch with a spot at the centre of the first 2D spot mode exhibits a well pronounced effect of normal current density. The latter may be interpreted as a manifestation of coexistence of a hot phase, representing the 1D abnormal mode, with a cold phase, representing a situation where no discharge is present at the point of the cathode surface being considered. The number of existing 2D modes decreases with a decrease in the radius $R$ of the discharge tube; there are only two modes at $R = 0.5$ mm.

When diffusion losses are taken into account, the number of multiple solutions is significantly reduced: only three 2D modes exist at $R = 1.5$ mm. One is the fundamental mode, comprising the Townsend, subnormal, normal and abnormal discharges. The first and second non-fundamental 2D modes are associated with patterns with an interior ring spot and, respectively, a spot at the centre and an interior ring spot. Only the fundamental mode was found at $R = 0.5$ mm.

The above-described pattern of self-organization in dc glow discharges without diffusion losses is typical for bistable nonlinear dissipative systems; in fact, it was predicted on these grounds [2]. In particular, there is a similarity with a classic problem of coexistence of fluid and vapour described by the

van der Waals equation and Maxwell's rule: the von Engel and Steenbeck solution, which is 1D and exists at all currents, may be viewed as an analogue of the solution of the van der Waals equation, while the bifurcating 2D solution which describes the normal discharge and exists in a limited current range may be viewed as an analogue of a solution which describes states with coexisting fluid and vapour and is governed by Maxwell's rule. The pattern of self-organization in dc glow discharges with diffusion losses is dramatically different: the normal discharge represents a section of the fundamental mode, i.e. the mode which exists at all discharge currents. This change in patterns is non-trivial and is analysed elsewhere [24].

Obviously, this modelling represents just the first step; further work is required in order to make a meaningful quantitative comparison with the experiment [9–13] possible. It seems, however, that the patterns with multiple spots represent axially symmetric analogues of the 3D patterns observed in [9–13]. Thus, the present modelling supports the hypothesis [14] that patterns with multiple spots may be described in the framework of basic mechanisms of glow discharge, so there is no need to introduce special mechanisms to this end.

Observations of axially symmetric self-organization patterns on cathodes of dc glow discharges have not been reported up to now. (Although axially symmetric patterns have been observed in gas discharges in other situations, e.g. on anode of glow discharge [27, 28] and in dielectric-barrier discharge [29].) The results obtained in this work suggest that solutions describing axially symmetric self-organized patterns in dc glow discharges do exist, although the question of their stability remains open, and it would be interesting to look for these patterns in the experiment.

Future work should include finding multiple 3D solutions, an investigation of stability of different steady-state solutions, and an introduction of more complex effects, such as the presence of multiple ion and/or neutral species, variations of the electron and heavy particle temperatures, non-locality of the electron transport (similarly to how it is done, e.g. in [7, 8, 30]). After this, a quantitative comparison with the observations [9–13] will become possible. In particular, the theory will have to explain why patterns with multiple spots are observed in xenon microdischarges and not in other discharges, and also to predict other conditions under which patterns can be observed in experiments. The analysis of stability will allow one to establish a relation with theoretical and experimental investigation of subnormal oscillations; e.g. [7, 31, 32] and references herein.

Finding of multiple 3D solutions may be facilitated by bifurcation analysis in a similar way as was done in this work while finding multiple 2D solutions. As an example, bifurcation points at which the two initial 3D modes branch off from the fundamental mode are shown by open circles in figure 3(*a*). One can see, in particular, that the 3D modes exist in a wider range of discharge currents than the 2D modes.

Preliminary results of numerical investigation of stability without account of diffusion losses indicated that the fundamental mode is stable except at the section between the bifurcation points of the first 3D mode, in agreement with the theory [24]. Results on stability of the 2D modes conform to the theory [24] in the vicinity of the bifurcation points, as they should, and reveal alternations of stability of a steady-state 2D mode against the same 3D perturbation mode, including against the first and second ones. Due to this phenomenon, the first 2D mode is stable in certain ranges of electric current, in contrast to what has been found in the case of the arc discharge, where the first 2D steady-state mode is always unstable [33].

## Acknowledgments

The work was performed within the activities of the project PTDC/FIS/68609/2006 *Cathode spots in high-pressure dc gas discharges: self-organization phenomena* of FCT, POCI 2010 and FEDER and of the project *Centro de Ciências Matemáticas* of FCT, POCTI-219 and FEDER. PGCA and MJF appreciate PhD fellowships from FCT, grants SFRH/BD/30598/2006 and SFRH/BD/35883/2007.

## References

[1] Raizer Yu P 1991 *Gas Discharge Physics* (Berlin: Springer)
[2] Benilov M S 1988 *Sov. Phys.—Tech. Phys.* **33** 1267–70
[3] Boeuf J P 1988 *J. Appl. Phys.* **63** 1342–9
[4] Raizer Yu P and Surgikov S T 1988 *High Temp.* **26** 428–35
[5] Fiala A, Pitchford L C and Boeuf J P 1994 *Phys. Rev.* E **49** 5607
[6] Kolobov V I and Fiala A 1994 *Phys. Rev.* E **50** 3018–32
[7] Arslanbekov R R and Kolobov V I 2003 *J. Phys. D: Appl. Phys.* **36** 2986–94
[8] Surzhikov S T 2005 *High Temp.* **43** 825–42
[9] Schoenbach K H, Moselhy M and Shi W 2004 *Plasma Sources Sci. Technol.* **13** 177–85
[10] Moselhy M and Schoenbach K H 2004 *J. Appl. Phys.* **95** 1642–9
[11] Takano N and Schoenbach K H 2006 *Plasma Sources Sci. Technol.* **15** S109–S117
[12] Lee B J, Rahaman H, Frank K, Mares L and Biborosch D L 2007 *Proc. 28th ICPIG (Prague, July 2007)* ed J Schmidt *et al* (Prague: Institute of Plasma Physics AS CR) pp 900–2
[13] Zhu W, Takano N, Schoenbach K H, Guru D, McLaren J, Heberlein J, May R and Cooper J R 2007 *J. Phys. D: Appl. Phys.* **40** 3896–906
[14] Benilov M S 2007 *Plasma Sources Sci. Technol.* **16** 422–5
[15] Rafatov I R, Šijačić D D and Ebert U 2007 *Phys. Rev.* E **76** 036206
[16] Benilov M S 2008 *Phys. Rev.* E **77** 036408
[17] Stollenwerk L, Amiranashvili S, Boeuf J P and Purwins H G 2006 *Phys. Rev. Lett.* **96** 255001
[18] Kim H C, Iza F, Yang S S, Radmilovic-Radjenovic M and Lee J K 2005 *J. Phys. D: Appl. Phys.* **38** R283–R301
[19] http://fisica.uma.pt/public/
[20] Biondi M A and Chanin L M 1954 *Phys. Rev.* **94** 910–6
[21] Hagelaar G J M and Pitchford L C 2005 *Plasma Sources Sci. Technol.* **14** 722–33
[22] Meunier J, Belenguer P and Boeuf J P 1995 *J. Appl. Phys.* **78** 731–45
[23] Fridman A and Kennedy L A 2004 *Plasma Phys. Eng.* (New York: Taylor and Francis)
[24] Almeida P G C, Benilov M S, Cunha M D and Faria M J 2009 *J. Phys. D: Appl. Phys.* **42** 194010
[25] Benilov M S 1992 *Phys. Rev.* A **45** 5901–12
[26] Haken H 1978 *Synergetics, An Inroduction* (*Springer Series in Synergetics* vol 1) (Berlin: Springer)
[27] Thomas C H and Duffendack O S 1930 *Phys. Rev.* **35** 72–91

[28] Müller K G 1988 *Phys. Rev.* A **37** 4836–45
[29] Gurevich E L, Zanin A L, Moskalenko A S and Purwins H G 2003 *Phys. Rev. Lett.* **91** 154501
[30] Boeuf J P, Pitchford L C and Schoenbach K H 2005 *Appl. Phys. Lett.* **86** 071501
[31] Kaganovich I D, Fedotov M A and Tsendin L D 1994 *Tech. Phys.* **39** 241–6
[32] Phelps A V 2001 *Plasma Sources Sci. Technol.* **10** 329–43
[33] Benilov M S and Faria M J 2007 *J. Phys. D: Appl. Phys.* **40** 5083–97